Angiogenic patterning by STEEL, an endothelial-enriched long noncoding RNA

H. S. Jeffrey Man[a,b], Aravin N. Sukumar[a,b], Gabrielle C. Lam[c,d], Paul J. Turgeon[b,e], Matthew S. Yan[b,f], Kyung Ha Ku[b,e], Michelle K. Dubinsky[a,b], J. J. David Ho[b,f], Jenny Jing Wang[b,e], Sunit Das[g,h], Nora Mitchell[i], Peter Oettgen[i], Michael V. Sefton[c,d,j], and Philip A. Marsden[a,b,e,f,1]

[a]Institute of Medical Science, University of Toronto, Toronto, ON M5S 1A8, Canada; [b]Keenan Research Centre for Biomedical Science in the Li Ka Shing Knowledge Institute, St. Michael's Hospital, University of Toronto, Toronto, ON M5B 1T8, Canada; [c]Donnelly Centre for Cellular and Biomolecular Research, University of Toronto, Toronto, ON M5S 3E2, Canada; [d]Institute of Biomaterials and Biomedical Engineering, University of Toronto, Toronto, ON M5S 3G9, Canada; [e]Department of Laboratory Medicine and Pathobiology, University of Toronto, Toronto, ON M5S 1A8, Canada; [f]Department of Medical Biophysics, University of Toronto, Toronto, ON M5G 1L7, Canada; [g]Arthur and Sonia Labatt Brain Tumour Research Institute, Hospital for SickKids, University of Toronto, Toronto, ON M5G 1X8, Canada; [h]Division of Neurosurgery and Keenan Research Centre for Biomedical Science, St. Michael's Hospital, University of Toronto, Toronto, ON M5B 1W8, Canada; [i]Department of Medicine, Beth Israel Deaconess Medical Center, Harvard Medical School, Boston, MA 02115; and [j]Department of Chemical Engineering and Applied Chemistry, University of Toronto, Toronto, ON M5S 3E5, Canada

Edited by Napoleone Ferrara, University of California, San Diego, La Jolla, CA, and approved January 24, 2018 (received for review August 28, 2017)

Endothelial cell (EC)-enriched protein coding genes, such as endothelial nitric oxide synthase (eNOS), define quintessential EC-specific physiologic functions. It is not clear whether long noncoding RNAs (lncRNAs) also define cardiovascular cell type-specific phenotypes, especially in the vascular endothelium. Here, we report the existence of a set of EC-enriched lncRNAs and define a role for spliced-transcript endothelial-enriched lncRNA (STEEL) in angiogenic potential, macrovascular/microvascular identity, and shear stress responsiveness. STEEL is expressed from the terminus of the HOXD locus and is transcribed antisense to HOXD transcription factors. STEEL RNA increases the number and integrity of de novo perfused microvessels in an in vivo model and augments angiogenesis in vitro. The STEEL RNA is polyadenylated, nuclear enriched, and has microvascular predominance. Functionally, STEEL regulates a number of genes in diverse ECs. Of interest, STEEL up-regulates both eNOS and the transcription factor Kruppel-like factor 2 (KLF2), and is subject to feedback inhibition by both eNOS and shear-augmented KLF2. Mechanistically, STEEL up-regulation of eNOS and KLF2 is transcriptionally mediated, in part, via interaction of chromatin-associated STEEL with the poly-ADP ribosylase, PARP1. For instance, STEEL recruits PARP1 to the KLF2 promoter. This work identifies a role for EC-enriched lncRNAs in the phenotypic adaptation of ECs to both body position and hemodynamic forces and establishes a newer role for lncRNAs in the transcriptional regulation of EC identity.

long noncoding RNA | endothelium | angiogenesis | hemodynamics | chromatin

A better understanding of how endothelial cells (ECs) acquire distinct phenotypes is a prerequisite for treatment of vascular diseases and for regenerative medicine purposes. EC-enriched genes are major determinants of specialized EC functions that coordinate EC phenotype to functional context such as microvascular versus macrovascular function (1).

Recent evidence from genome-wide transcription analysis suggests that long noncoding RNAs (lncRNAs) play important roles in controlling cellular phenotype (2–4) and in pathogenesis of disease, including cancer and cardiovascular disease (4, 5). Still, only few cell type-enriched lncRNAs have been functionally characterized (2). Though some lncRNAs are tissue specific (2), others, such as the lncRNA MALAT1, are widely expressed and serve core cellular functions in multiple cell types (6). In ECs, many of the genes that define endothelial phenotype, including control of vasomotor tone, response to shear stress, and formation of new blood vessels, are expressed in an EC-enriched fashion (1). Of interest, EC-enriched lncRNAs have yet to be described. We sought to identify EC-enriched lncRNAs that could contribute to the phenotypic plasticity of ECs in their unique environment.

In this study, we describe a set of EC-enriched lncRNAs and functionally characterize spliced-transcript endothelial-enriched lncRNA (STEEL). We demonstrate that STEEL promotes network formation in vitro and blood vessel formation in vivo. STEEL regulates transcription of a key mediator of local blood flow, endothelial nitric oxide synthase (eNOS), and a key sensor of hemodynamic forces, Kruppel-like factor 2 (KLF2). The STEEL RNA forms a ribonucleoprotein complex with poly(ADP-ribose) polymerase 1 (PARP1) that targets PARP1 to the KLF2 and eNOS promoters. We argue that feedback inhibition regulates STEEL expression to modulate angiogenic behavior in a vascular tree position-dependent and shear-dependent fashion.

Results

Cell Type-Specific Expression of lncRNAs and Protein-Coding mRNAs in Human Primary Cells. Six primary human cell types [human umbilical vein ECs (HUVECs), human dermal microvascular ECs (HMVECs), human aortic smooth muscle cells (HASMCs), hepatocytes, dermal fibroblasts, and epidermal keratinocytes] from multiple independent donors were profiled, in parallel, for

Significance

Endothelial cells (ECs) form the inner cellular lining of blood vessels and are necessary in the establishment and maintenance of the closed cardiovascular system, especially the physiology of regulated blood flow to and from tissues. Recently, long noncoding RNAs (lncRNAs) have been described to have roles in gene regulation for a variety of processes, including stem cell functions and differentiation of stem cells into tissues. This work identifies lncRNAs that are enriched in ECs and further characterizes the lncRNA, spliced-transcript endothelial-enriched lncRNA (STEEL). STEEL promotes the formation of intact blood vessels by ECs in vivo. Moreover, STEEL regulates transcription of a key mediator of local blood flow, endothelial nitric oxide synthase (eNOS), and a key sensor of hemodynamic forces, Kruppel-like factor 2 (KLF2).

Author contributions: H.S.J.M. and P.A.M. designed research; H.S.J.M., A.N.S., G.C.L., P.J.T., M.S.Y., K.H.K., M.K.D., J.J.D.H., J.J.W., N.M., and P.O. performed research; M.V.S. contributed new reagents/analytic tools; H.S.J.M., A.N.S., G.C.L., P.J.T., M.S.Y., K.H.K., M.K.D., S.D., M.V.S., and P.A.M. analyzed data; and H.S.J.M. and P.A.M. wrote the paper.

The authors declare no conflict of interest.

This article is a PNAS Direct Submission.

Data deposition: The data reported in this paper have been deposited in the Gene Expression Omnibus (GEO) database, https://www.ncbi.nlm.nih.gov/geo (accession no. GSE108321). The mass spectrometry proteomics data have been deposited to the ProteomeXchange Consortium via the PRIDE partner repository with the dataset identifier PXD008581.

[1]To whom correspondence should be addressed. Email: p.marsden@utoronto.ca.

This article contains supporting information online at www.pnas.org/lookup/suppl/doi:10.1073/pnas.1715182115/-/DCSupplemental.

Published online February 21, 2018.

the expression of lncRNAs and protein-coding genes using custom lncRNA microarrays representing 23,155 putative lncRNAs and 19,484 protein-coding genes (Fig. 1 *A–C*, *SI Appendix*, Figs. S1 and S2, and Dataset S1). Of those, 18,524 lncRNAs and 18,701 protein-coding genes were expressed above the 20th percentile in at least one cell type and were considered for further analysis. A total of 2,974 lncRNAs (16.1%) and 5,276 protein-coding genes (28.2%) were differentially expressed across cell types. Consistent with this observation, unsupervised clustering using Pearson centered correlation revealed cell type-based patterns of expression for both lncRNAs and protein-coding mRNAs (Fig. 1*A* and *SI Appendix*, Fig. S2*A*).

Identification of Endothelial-Enriched lncRNAs. HUVEC and HMVEC lncRNAs and protein-coding genes cluster on heatmap and principal component analyses (Fig. 1 *A* and *B* and *SI Appendix*, Figs. S1*A* and S2*A*). We defined EC-enriched lncRNAs as those that were enriched greater than fourfold (*SI Appendix*, Fig. S1*B*) in either HUVECs or HMVECs versus each of the four non-EC types, with significance by one-way ANOVA. This analysis yielded 116 EC-enriched lncRNAs: 29 EC-enriched lncRNAs in common between HUVECs and HMVECs, 28 and 59 enriched uniquely in either HUVECs or HMVECs, respectively (Fig. 1*D* and Dataset S1). By comparison, we found 234 EC-enriched protein-coding mRNAs: 86 EC-enriched protein-coding mRNAs in common between HUVECs and HMVECs, and 45 and 103 protein-coding mRNAs enriched uniquely in either HUVECs or HMVECs, respectively (*SI Appendix*, Fig. S1*D*). EC-enriched protein-coding genes including VE-cadherin, vWF, and CD31/PECAM1 (1) are highly EC enriched on the microarrays (*SI Appendix*, Fig. S2 *B–D*). We verified representative EC-enriched lncRNAs that were highly enriched and abundant, spliced, did not have sense overlap with protein-coding genes, and were near EC-enriched protein-coding genes. HHIP-AS1, FLI-AS1, LOC100505812/CARD8-AS, AF161442/HSPC324, and STEEL (*SI Appendix*, Fig. S3) are lncRNAs transcribed antisense to and nonoverlapping with EC-enriched genes HHIP1, FLI1, CARD8, EGFL7, and HOXD1 (Dataset S1) (1). We also defined a group of "EC exempt" lncRNAs and protein-coding mRNAs as those whose expression was decreased by greater than fourfold in both HUVECs and HMVECs versus each of the other four cell types. This analysis identified 25 lncRNAs and 113 protein-coding mRNAs as EC exempt (*SI Appendix*, Fig. S4 and Dataset S2). Whether any of these lncRNAs silence EC-enriched genes in other cell types, similar to the RE-1 silencing transcription factor, which silences neuronal genes in nonneuronal cells (7), requires further study.

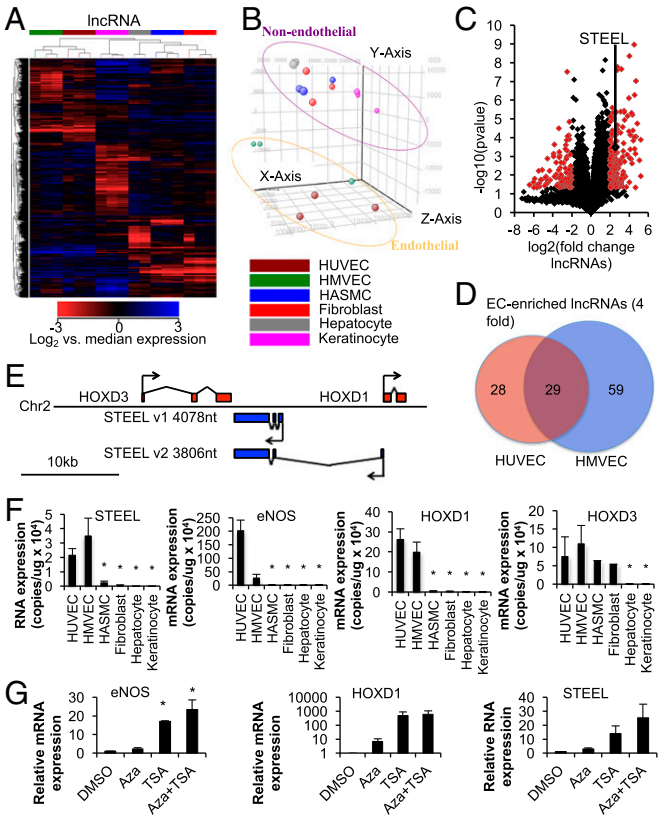

Fig. 1. Endothelial-enriched expression of lncRNAs. (*A* and *B*) Heatmap (*A*) and principal component analysis (*B*) of lncRNA expression across multiple samples in six human cell types. $n = 3$ except for hepatocyte ($n = 2$). (*C*) Volcano plots showing differential expression of lncRNAs in endothelial cells vs. nonendothelial cells. (*D*) Venn diagrams showing EC-enriched lncRNAs with fourfold or higher enrichment. (*E*) Schematic representation of the distal end of the HOXD locus. Red, protein-coding genes; blue, lncRNAs. (*F*) RT-qPCR of STEEL, eNOS, HOXD1, and HOXD3. (*G*) RT-qPCR of eNOS, HOXD1, and STEEL expression in HASMCs after treatment with 5-Aza-2′-deoxycytidine (Aza) and Trichostatin A (TSA). *$P < 0.05$ vs. ECs. Error bars represent SEM.

STEEL Is an Endothelial-Enriched lncRNA. Our main objective was to identify a lncRNA that has a functional role in ECs. Human homeobox protein-coding genes (HOX) exist as 39 gene family members on four chromosomes and are critical for axial patterning and maintenance of positional identity (3, 8). HOX lncRNAs have been used as a model for understanding lncRNA function and mechanisms (2–4). As a result, we chose STEEL (also known as GenBank accession no. NR_110458, HOXD-AS1, and HAGLR), a spliced and polyadenylated lncRNA transcribed in an antisense direction and positioned in the intergenic region between the HOXD1 and HOXD3 loci, for further characterization (Fig. 1*E* and *SI Appendix*, Figs. S5 *A–D* and S6*C*). The major variant is 4,078 nt in length and encoded by three exons. No sequences contain repetitive mobile DNA elements. HOXD1 and two variants of STEEL were found to have expression patterns highly specific to ECs, while other HOX paralogous group 1 genes were not (Fig. 1*F* and *SI Appendix*, Figs. S2 *E* and *F* and S3 *E–G*), despite the oft reported functional redundancy between HOX loci (8). Both STEEL and HOXD1 were especially enriched in microvascular HMVECs (9). While HOXD3 was enriched in mesenchyme, it was less specific to ECs. Expression levels of STEEL RNA are low (in HUVEC ~1/10, in HMVEC ~1/5 compared with the adjacent gene HOXD1). STEEL is expressed across diverse human tissues, with particular enrichment in the testis and kidney (*SI Appendix*, Fig. S7 *A* and *B*). HOTAIR, which is expressed from the HOXC locus and represses genes in the HOXD locus, is relatively depleted in ECs (*SI Appendix*, Fig. S4*B*) (3).

To assess the mechanisms of EC-enriched expression of STEEL, we treated HASMCs with 5-Aza-2′-deoxycytidine (Aza) and Trichostatin A (TSA) to inhibit DNA methylation and histone deacetylation, respectively. As we have previously reported for eNOS, and shown for comparison, both HOXD1 and STEEL are epigenetically repressed in nonexpressing cell types (Fig. 1*G*) (10).

Bioinformatic and Experimental Data Indicate that STEEL Is a Noncoding RNA. Most lncRNAs are expected to contain an ORF of at least 100 aa by chance alone and true coding regions tend to be much longer than expected by chance (11). While a clear-cut distinction between coding and noncoding RNAs may not exist (11), analysis of ORF length, ORF homology, and coding potential calculator score (12) indicate that STEEL is unlikely to be protein coding (*SI Appendix*, Fig. S5*E*). Experimental evidence supports noncoding functions. STEEL contains nuclear localization sequences (13) and, similar to Xist, is located primarily in the nucleus (*SI Appendix*, Fig. S6 *A* and *B*) (14, 15). Polyribosome profiling shows that Cyclophilin A mRNA was associated with polyribosomes, whereas STEEL was not (*SI Appendix*, Fig. S6*D*). Taken together, these data support the annotation of STEEL as a lncRNA.

STEEL RNA Modulates Endothelial Network Formation and Migration in Vitro. To assess the functional role of STEEL, we performed gain-of-function (overexpression) and loss-of-function (siRNA knockdown) experiments in HUVECs using Matrigel network formation assays. We assessed STEEL gain of function using integrating lentivirus containing enhanced GFP (eGFP) alone (control), or both STEEL and eGFP (STEEL) as separate transcription units with, on average, a 15-fold increase in STEEL expression (*SI Appendix*, Fig. S8), and found increased connectivity between cells (total "networks" and "branch points") (Fig. 2 *A* and *B*). We then assessed STEEL loss of function using siRNA and found decreased network formation in Matrigel (Fig. 2*B*). To assess how STEEL mediates increased network formation, we performed EC migration and proliferation assays. A monolayer scratch assay showed decreased wound recovery at 24 h after denudation with STEEL knockdown (*SI Appendix*, Fig. S9 *A* and *B*). Furthermore, we assessed the effect of STEEL on EC proliferation in HUVECs using two independent methods. First, we used carboxyfluorescein succinimidyl ester (CFSE) labeling of in vitro cells to trace multiple generations of ECs using dye dilution by flow cytometry. CFSE labels cytosolic proteins (lysine and other amine groups). STEEL overexpression promotes dye dilution. In contrast, STEEL knockdown studies showed inhibition of dye dilution. Next, we assessed DNA synthesis by BrdU incorporation and found that STEEL knockdown led to decreased DNA synthesis (*SI Appendix*, Fig. S10 *A–C*). Furthermore, STEEL knockdown decreased apoptosis as assessed by Caspase 3 activity (*SI Appendix*, Fig. S10*D*). These in vitro results suggest that EC expression of STEEL promotes new blood vessel formation by cellular turnover, migration, and network formation.

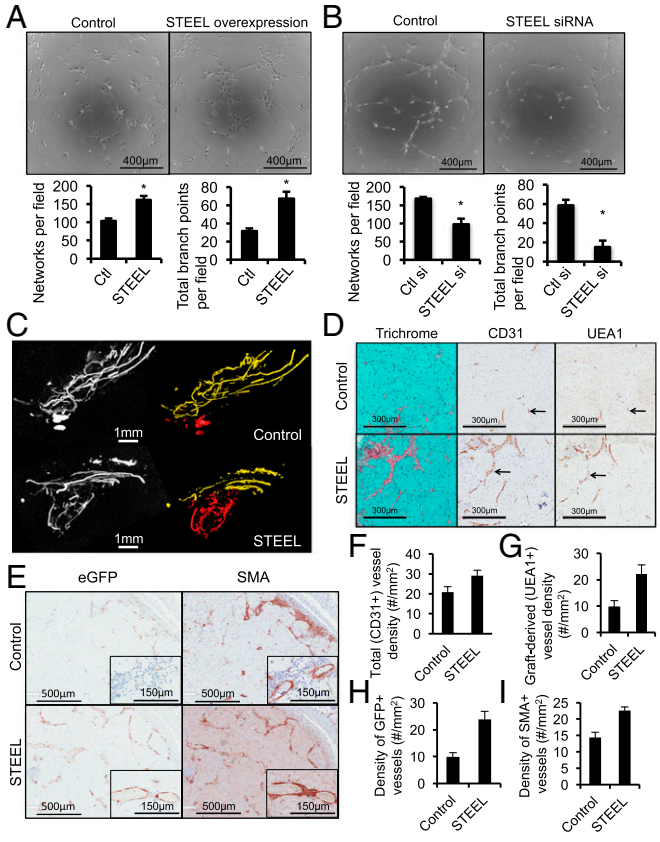

Fig. 2. STEEL RNA promotes network formation in vitro and angiogenesis in vivo. (*A*) HUVECs transduced with lentivirus containing eGFP alone or STEEL/eGFP imaged after 6 h of growth on Matrigel. (*B*) HUVECs transfected with Ctl siRNA (nontargeting sequence) and STEEL siRNA imaged after 6 h of growth on Matrigel. (*C*) Contrast microCT images of implants from mice at day 21. Red, implant vessels; yellow, skin vessels. (*D* and *E*) Immunohistochemistry stain of FFPE sections from modules at day 14 containing HUVECs and human adMSCs embedded in collagen and implanted into SCID/Bg mice. *Inset* boxes in *E* represent ~3.4× magnification. (*F–I*) Quantitation of CD31 (*F*), UEA1 (*G*), GFP (*H*), and SMA (*I*) positive vessels. **P* < 0.05. Error bars represent SEM.

STEEL RNA Increases Blood Vessel Formation in Vivo. We used a tissue engineering approach to assess a role of STEEL in angiogenesis in vivo. This approach offers the potential for practical application of findings, especially in the area of regenerative medicine (16). Collagen modules embedded with adipose mesenchymal stromal cells (adMSCs) were coated with a monolayer of transduced HUVECs and implanted into immunologically deficient SCID/Bg mice. MicroCT imaging of implants at 21 d postimplantation showed the development of internal vascular networks in the implanted collagen modules that were connected to host vasculature (Fig. 2*C*, *SI Appendix*, Fig. S11 *A* and *B*, and Movies S1 and S2). The STEEL-transduced implants exhibited greater density of perfused vessels. Control implants had reduced vessel formation as well as extravasation and pooling of contrast. Immunohistochemistry (IHC) performed on fresh-frozen and paraffin embedded (FFPE) modules 14 d postimplantation showed an increase in the total number of vessels (the CD31 antibody stains both mouse and human), which were composed mainly of human STEEL-transduced ECs (UEA1 and GFP staining) rather than mouse ECs (Fig. 2 *D*, *F*, and *G*). Furthermore, STEEL implants had greater numbers of vessels that were surrounded by cells stained by smooth muscle actin (SMA), indicating greater vessel maturation surrounding the STEEL-transduced HUVECs (Fig. 2 *E*, *H*, and *I*). These results suggest that STEEL RNA promotes the development of functional blood vessels by ECs within avascular modules.

STEEL RNA Regulates Gene Expression in ECs. STEEL loss of function with two independent siRNAs identified target genes in both HUVECs and HMVECs (Fig. 3 *A* and *B*, *SI Appendix*, Fig. S12 *A–G*, and Dataset S3). A total of 225 protein-coding genes were down-regulated and 80 were up-regulated when both EC types were grouped for analysis. In HMVECs alone, 544 protein-coding genes were down-regulated and 218 were up-regulated. In HUVECs alone, 177 protein-coding genes were down-regulated and 125 were up-regulated by STEEL knockdown by twofold, respectively. The number of STEEL target genes is comparable to many other long intergenic noncoding RNAs that exert regulatory effects on gene expression (3, 4). STEEL regulated 6/86 (~7%) of EC-specific genes in common between HUVECs and HMVECs, 4/103 (~4%) of HMVEC-only enriched genes, and 2/45 (~4%) of HUVEC-only enriched genes (*SI Appendix*, Fig. S12 *B–D*).

Unlike the lncRNA HOTTIP (17), a lncRNA that coordinates the activation of several 5′ HOXA genes *in cis*, STEEL affected RNA expression primarily *in trans*. The two genes flanking STEEL, HOXD1 and HOXD3, did not show significant changes in RNA or protein levels with STEEL knockdown (Fig. 3 *C* and *D*). Unlike HOTAIR, which regulates a large domain of genes in the HOXD locus *in trans* (3), STEEL knockdown did not target a unique domain of genes within the other HOX loci, though some HOX proteins were targeted in individual cell types (*SI Appendix*, Fig. S12 *E* and *F*). Knockdown of HOXD1 showed that STEEL expression is not regulated *in cis* (*SI Appendix*, Fig. S12*H*), though functional interaction and rescue from other HOX paralogous group 1 genes is not excluded. STEEL knockdown decreased genes of biological interest in ECs, especially KLF2, a key sensor of hemodynamic forces, and eNOS, a key mediator of vasomotor tone (Fig. 3*E*) (18, 19).

STEEL RNA Regulates Transcription and Chromatin of Select Target Genes. Because STEEL RNA is primarily in the nucleus, we asked whether the STEEL RNA regulates target gene transcription. Indeed, heterogenous nuclear RNA levels (hnRNA/pre-mRNA) and RNA polymerase II loading at the proximal promoters of KLF2 and eNOS decreased after STEEL knockdown (Fig. 3 *G* and

CELL BIOLOGY

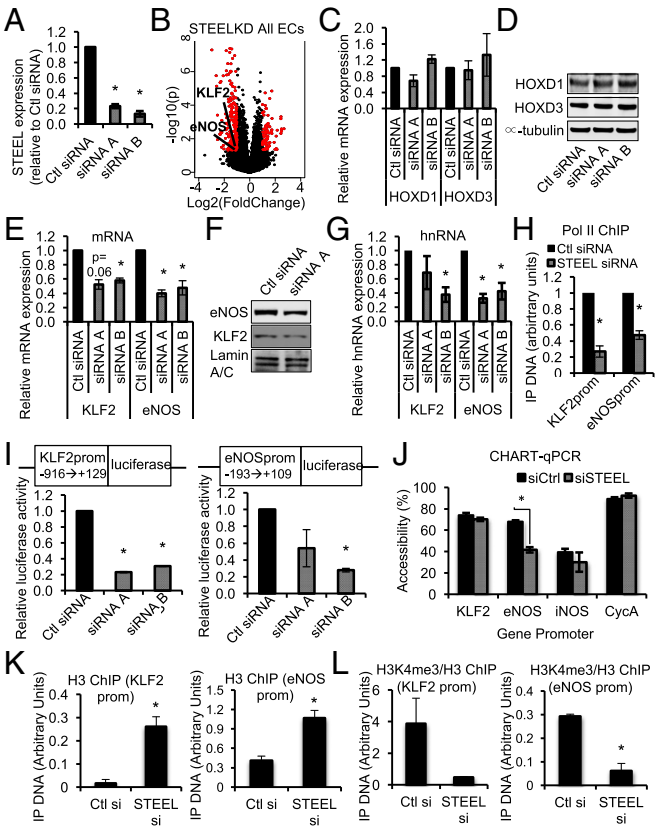

Fig. 3. Gene regulation in endothelial cells by STEEL RNA. (*A*) RT-qPCR of STEEL knockdown by two independent siRNA sequences. (*B*) Volcano plot representing mRNAs regulated by STEEL knockdown in HUVECs and HMVECs from microarray. Red indicates differentially regulated genes. (*C*–*F*) RT-qPCR of HOXD1 and HOXD3 mRNA with STEEL knockdown. (*D*) Western blot of HOXD1 and HOXD3 protein with STEEL knockdown. (*E*) RT-qPCR of KLF2 and eNOS mRNA with STEEL knockdown. (*F*) Western blot of KLF2 and eNOS protein with STEEL knockdown. (*G*) RT-qPCR of KLF2 and eNOS hnRNA (pre-mRNA) with STEEL knockdown. (*H*) RT-qPCR of RNA Pol II ChIP at KLF2 and eNOS promoters. (*I*) Promoter luciferase-reporter assays with STEEL knockdown. (*J*) CHART-qPCR with STEEL knockdown. (*K* and *L*) ChIP-qPCR of the core histone, histone H3, and the activating epigenetic mark histone 3 lysine 4 trimethyl (H3K4me3) at the KLF2 and eNOS promoters after STEEL siRNA knockdown in HUVECs. $*P < 0.05$. Error bars represent SEM.

H). Moreover, promoter luciferase-reporter assays for KLF2 and eNOS (Fig. 3*I*) reveal decreased KLF2/eNOS promoter activity with STEEL knockdown. To assess for epigenetic changes as a cause for these transcriptional changes, we used chromatin accessibility qPCR (CHART-qPCR) and found that STEEL knockdown decreased chromatin accessibility at the eNOS promoter and STEEL overexpression increased chromatin accessibility at the KLF2 promoter (Fig. 3*J* and *SI Appendix*, Fig. S13). To extend these results, we also assessed nucleosome occupancy at both the eNOS and KLF2 promoters by chromatin immunoprecipitation of core histone H3, and found increased nucleosome occupancy at both the KLF2 and eNOS promoters with STEEL knockdown (Fig. 3*K*). We also found a decrease in the activating mark, histone 3 lysine 4 trimethylation (H3K4me3), at both the KLF2 and eNOS promoters with STEEL knockdown (Fig. 3*L*) in HUVECs.

Feedback Inhibition of STEEL by KLF2 and eNOS in the Presence and Absence of Laminar Flow. Despite up-regulating basal eNOS expression (Fig. 3 *E* and *F*), we note that STEEL expression is greater in microvascular ECs (HMVECs), while eNOS expression is greater in macrovascular ECs (HUVECs) (Fig. 1 *A* and *B*). We hypothesized that there may be feedback inhibition by eNOS on STEEL RNA expression. Accordingly, siRNA knockdown of eNOS increased STEEL RNA expression in HUVECs (Fig. 4*G*).

As noted by others, both eNOS and KLF2 are up-regulated by laminar flow (Fig. 4*A*) (20). We found decreased STEEL RNA and hnRNA with laminar flow (~10 dynes/cm^2) at 48 h, following up-regulation of both KLF2 and eNOS mRNA (Fig. 4 *B* and *C* and *SI Appendix*, Fig. S14*A*). We postulated that KLF2, a major flow-induced transcriptional regulator, may contribute to STEEL and HOXD1 regulation during laminar flow. Indeed, overexpression of mouse KLF2 for 48 h in HUVECs in static conditions decreased STEEL RNA/hnRNA and HOXD1 mRNA (Fig. 4 *D*–*F* and *SI Appendix*, Fig. S14*B*). Moreover, siRNA depletion of KLF2 in the presence of laminar flow increased STEEL RNA (*SI Appendix*, Fig. S14*C*). These regulatory loops may be relevant in disease settings, as decreased STEEL expression was observed when HUVECs were exposed to flow patterns that modeled "atheroprotective" flow compared with disturbed "atheroprone" flow (Fig. 4*H*) (21). Even though STEEL knockdown reduces basal KLF2 expression, STEEL knockdown did not reduce KLF2 induction by laminar flow. In contrast, STEEL knockdown decreased KLF4 induction by laminar flow (*SI Appendix*, Fig. S14 *C* and *D*). Taken together, these findings suggest that: (*i*) STEEL functions to maintain basal expression of KLF2 and eNOS in the absence of flow and (*ii*) conditions that augment eNOS and KLF2 expression, such as laminar flow, repress STEEL expression. These observations provide a plausible molecular mechanism behind the increased expression of STEEL in microvascular beds versus large vessels such as the aorta and pulmonary artery (*SI Appendix*, Fig. S15) (22).

STEEL Regulation of Target Genes Is Modulated by Epigenetic State. We then assessed the effect of overexpressing STEEL above physiologic levels on target genes. In HUVECs, where STEEL is

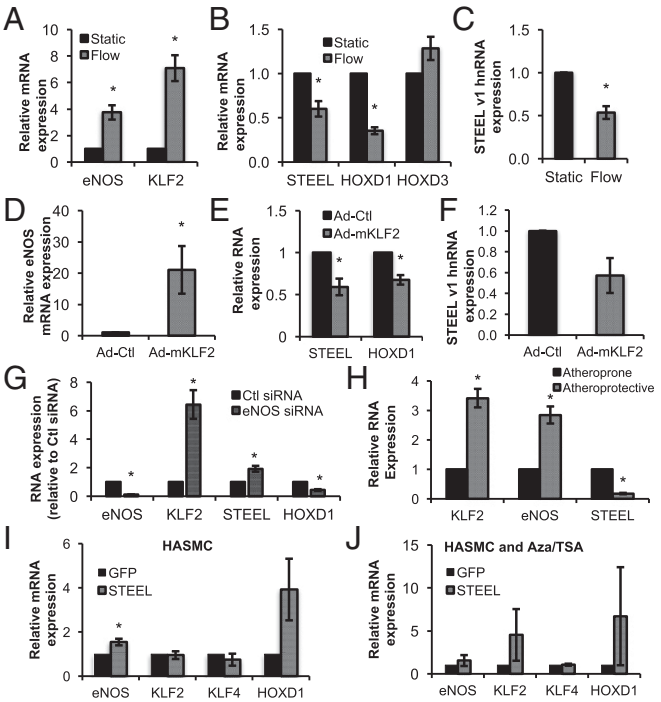

Fig. 4. Feedback inhibition of STEEL by KLF2 and eNOS. (*A*–*C*) RT-qPCR of KLF2, eNOS, STEEL, HOXD1, HOXD3 RNA, and STEEL hnRNA in HUVECs exposed to 48 h of laminar flow. (*D*–*F*) RT-qPCR of eNOS, STEEL, HOXD1 mRNA, and STEEL hnRNA with adenoviral overexpression of mouse KLF2 in HUVECs. (*G*) RT-qPCR of STEEL, KLF2, and HOXD1 expression with eNOS siRNA knockdown in HUVECs. (*H*) RT-qPCR of KLF2, eNOS, and STEEL in atheroprone and atheroprotective flow. (*I* and *J*) RT-qPCR of eNOS, KLF2, KLF4, and HOXD1 mRNA with STEEL overexpression in HASMCs with or without Aza/TSA. $*P < 0.05$. Error bars represent SEM.

already robustly expressed, negligible effects were noted with STEEL overexpression (~10-fold, from ~120 to ~1,200 copies per well) on eNOS and KLF2 mRNA expression (*SI Appendix*, Fig. S16 *A*, *C*, and *D*). Also, KLF4 and HOXD1 were not changed. In marked contrast, STEEL overexpression in nonexpressing cells (HASMCs), (~400-fold from ~4 to ~1,800 copies per well), affected target gene expression. We found a significant increase in eNOS and HOXD1 mRNA expression, but not KLF4 mRNA expression, with STEEL overexpression (Fig. 4*I* and *SI Appendix*, Fig. S16*B*). With epigenetic derepression by the addition of Aza and TSA, STEEL overexpression increased KLF2, but not KLF4, mRNA expression in HASMCs (Fig. 4*J*).

Discovery of STEEL RNA Binding Proteins. We compared RNA pulldown of nuclear proteins by polyA (23) RNA, the androgen receptor (AR) RNA, and STEEL RNA (Fig. 5 *A* and *B*). A total of 243 proteins were pulled down by at least one of these three RNAs, of which 175 were pulled down by STEEL RNA. We prioritized proteins whose normalized counts were enriched at least twofold in STEEL pulldowns versus all others and found that 66 were enriched or uniquely bound to STEEL RNA (*SI Appendix*, Fig. S17 *A* and *B* and Dataset S4). Twelve of these proteins were recently identified as binding partners for the Xist RNA (14) and others are known to interact with chromatin (Fig. 5*B*). We sought to confirm the in vitro associations of STEEL with the poly-ADP ribosylase, PARP1 because: (*i*) PARP1 was one of the most highly enriched binding proteins and was unique compared with Xist binding proteins; (*ii*) PARP1 is known to have gene regulatory function and is thought to be a regulator of epigenetic pathways (24); and (*iii*) STEEL bound multiple proteins in the PARP1 interactome (24). Native RNA immunoprecipitation (RIP) of PARP1 (Fig. 5 *C* and *D*) confirmed that STEEL RNA associated with PARP1 and not SNRNP70, a spliceosome protein. These reciprocal pulldowns show a specific interaction between STEEL RNA and PARP1 protein.

STEEL RNA Increases the Affinity of PARP1 at Target Chromatin Sites. One proposed mechanism of lncRNA function suggests that lncRNAs coordinate and/or localize regulatory proteins to genomic regions (14). We hypothesized that nuclear-enriched STEEL could recruit PARP1 protein to target promoters. PARP1 chromatin immunoprecipitation (ChIP) showed increased PARP1 occupancy at the KLF2 and eNOS promoters compared with the Cyclophilin A promoter (*SI Appendix*, Fig. S17*C*). Next, STEEL knockdown followed by PARP1 ChIP showed decreased PARP1 occupancy at the KLF2 and eNOS promoters following STEEL knockdown (Fig. 5 *E*–*G*). Importantly, a decrease in total cell PARP1 mRNA and protein levels with STEEL knockdown did not account for the decreased PARP1 occupancy in this setting (*SI Appendix*, Fig. S17 *D* and *E*). We also note that PARP1 mRNA levels were not affected by laminar flow or KLF2 overexpression in HUVECs, 1.09 ± 0.39 fold static vs. flow and 1.20 ± 0.80 fold in Ctl vs. KLF2 overexpression in HUVECs (mean ± SEM, $n = 5$). These results suggest that STEEL RNA interaction with PARP1 contributes to PARP1 association with target genomic loci.

Discussion

Endothelial heterogeneity is an important feature that adapts EC function to regional requirements of the closed cardiovascular system (22). Here, we identified an EC-enriched lncRNA, STEEL, that directs angiogenic patterning of ECs in response to vascular position and mechanical forces of the circulation. Specifically, we provide a molecular mechanism for the microvascular distribution of STEEL and HOXD1. STEEL increases EC migration, network formation in vitro, and microvascular network formation and integrity in vivo. Feedback inhibition by STEEL target genes eNOS and KLF2 suggests tight regulation of STEEL-induced phenotypes. Consistent with other studies (14), we found multiple STEEL ribonucleoproteins (RNPs). One STEEL RNP component, PARP1, was dependent on STEEL for localization at select genomic loci of STEEL target genes, eNOS and KLF2.

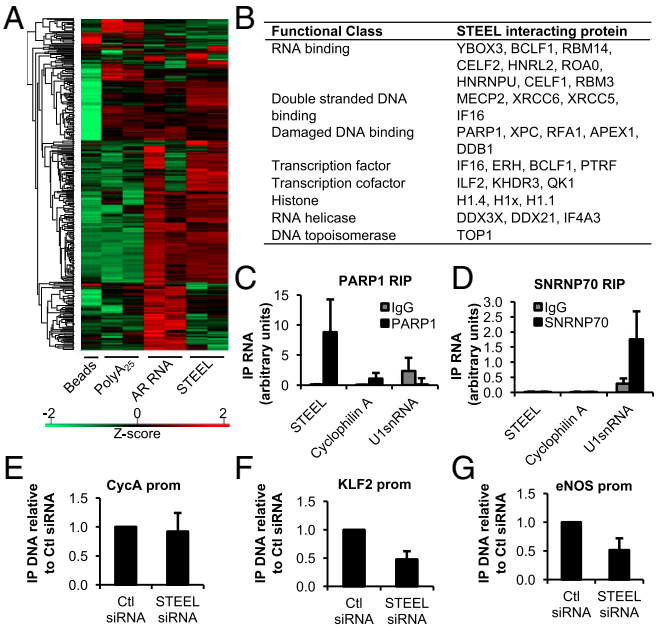

Functional Class	STEEL interacting protein
RNA binding	YBOX3, BCLF1, RBM14, CELF2, HNRL2, ROA0, HNRNPU, CELF1, RBM3
Double stranded DNA binding	MECP2, XRCC6, XRCC5, IF16
Damaged DNA binding	PARP1, XPC, RFA1, APEX1, DDB1
Transcription factor	IF16, ERH, BCLF1, PTRF
Transcription cofactor	ILF2, KHDR3, QK1
Histone	H1.4, H1x, H1.1
RNA helicase	DDX3X, DDX21, IF4A3
DNA topoisomerase	TOP1

Fig. 5. Discovery of functional STEEL ribonucleoprotein complexes. (*A*) Heatmap displaying protein interactions found using RNA pulldown with magnetic beads, polyA (23) RNA, AR RNA, and STEEL lncRNA. (*B*) Table of functional annotations of select STEEL-interacting proteins. (*C* and *D*) RNA immunoprecipitation targeting PARP1 and SNRNP70. (*E*–*G*) ChIP of PARP1 at the Cyclophilin A (CycA), KLF2, and eNOS promoters in the presence and absence of STEEL.

Though many transcription factors are expressed in ECs, an EC-enriched "master regulator" that maintains EC identity has not been identified (25). Epigenetic mechanisms maintain expression of EC-enriched genes such as eNOS; yet the factors that direct the EC-specific pattern of expression have yet to be identified (25). This work describes a set of EC-enriched lncRNAs and identifies functional roles for STEEL, a prototypic EC-enriched lncRNA. STEEL is expressed and regulates gene expression in a variety of human ECs and especially contributes to microvascular ECs. STEEL knockdown in HUVECs and HMVECs generated common and distinct target genes. We do not know whether this finding is a result of the differential expression of STEEL and STEEL RNPs between these cell types, though other factors such as chromatin state and basal expression levels of target genes appear to be influential. Similar observations are described for other lncRNAs. For example, the timed induction of the Xist lncRNA is critical for X inactivation in mammalian XX cells; yet the forced induction of Xist at distinct stages of development shows contrasting effects on Polycomb recruitment to the X chromosome (15).

This work shows that two genes from the HOXD cluster, STEEL and HOXD1, are EC enriched. Though patterns of HOX cluster expression can distinguish EC subtypes across the vasculature, including microvascular and macrovascular patterning (9), expression of HOX lncRNAs and proteins in an EC-enriched fashion has not been previously described. This collinear expression is a known phenomenon in HOX genes (8). We did not find evidence supporting *cis* cross-regulation between STEEL and HOXD1 in ECs, though *trans* regulation of HOXD1 by STEEL occurred in HASMCs, a setting in which STEEL was expressed outside its native locus and neither STEEL nor HOXD1 are normally expressed. As with STEEL, HOXD1 is thought to promote angiogenesis (23). Interestingly, the STEEL/HOXD1 locus contributes to species-specific nociceptor circuit patterning (26) and STEEL expression has been described in a neuroblastoma model (27), though it is not yet clear whether there is non-EC expression of STEEL in normal brain.

STEEL expression appears to be tightly regulated. Not only is STEEL EC enriched, but it is actively repressed, as is HOXD1, in nonexpressing cell types, such as aortic smooth muscle cells (HASMCs). Despite up-regulating both KLF2 and eNOS under basal conditions, STEEL is subject to feedback inhibition by both target genes. This tight regulation may reflect the importance of dosing to STEEL function. Physiologic shear stress, especially pulsatile flow, results in a quiescent endothelial phenotype, whereas abnormal shear stress, particularly low shear stress in disturbed flow, results in a more activated endothelial phenotype that includes increased proliferation and activation of inflammatory pathways (20). Regions of low shear stress are susceptible to the development of atherosclerosis and contribute to the notion that the response to low shear stress is mainly a determinant of disease (19, 20). Whether the functional role of increased expression of STEEL in atheroprone versus atheroprotective flow is advantageous or deleterious requires further study. We note that STEEL overexpression led to an increase in KLF2 expression and vessel maturity. Overexpression of KLF2 in static conditions, to levels comparable to laminar flow, inhibits angiogenesis, EC proliferation, and EC migration (18, 28). In contrast, STEEL promotes these processes. Our work indicates that KLF2 transcription is maintained by a lncRNA under static conditions and adds to the paradigm of flow regulation of KLF2 (21).

While many mechanisms of action for lncRNAs are proposed, few have been characterized (2, 14). Much early work has focused on epigenetic regulation and the ability of lncRNAs to recruit Polycomb proteins (3, 4, 14) and histone 3 lysine 27 trimethylation (H3K27me3). Interestingly, STEEL bound to PARP1, which does not have a known RNA binding domain (29), but is often a positive cofactor for transcriptional regulation through interaction with chromatin, chromatin modifiers, or transcription factors (24). Our work provides a description of a lncRNA interaction that mediates PARP1 occupancy at target genomic loci. PARP1 has been implicated in endothelial dysfunction and the development of atherosclerosis (24). Whether STEEL is a regulator of PARP1 function or PARP1 regulates STEEL function is not yet known.

Much progress has been made describing lncRNA expression, function, and mechanisms. This body of work highlights an emerging realization, namely that lncRNA expression and function can be cell-type specific. This work identifies STEEL as an EC-specific long noncoding RNA.

Materials and Methods

Microarray Analysis. Custom lncRNA microarrays on Arraystar Human lncRNA Microarray (Nimblegen 12 × 135 K array platform, 23,155 lncRNAs, 19,484 protein-coding genes) and Human lncRNA Microarray V2.0 (Agilent 8 × 60 K array platform, 33,045 lncRNA probes, 30,215 protein-coding mRNA probes) were used for cell specificity and STEEL knockdown experiments, respectively. All microarray data have been deposited in National Center for Biotechnology Information Gene Expression Omnibus (accession no. GSE108321).

Application of Shear Stress Using Parallel Plate Flow Chambers. A total of 750,000 HUVECs were seeded on 75 × 25 mm microscope slides (Thermo Fisher Scientific) coated with 0.2% gelatin. After 2–3 d of culture, a parallel plate flow apparatus was used to generate steady laminar flow of 10 dynes/cm^2 for 48 h (24 h for knockdown experiment).

Tissue Engineered Implants. Implants containing transduced HUVECs and adMSCs were prepared as previously described (*SI Appendix*, Fig. S11) (16). Immunohistochemistry of FFPE sections was performed at 14 d and microCT at 21 d. All animal experiments were approved by the University of Toronto Faculty of Medicine Animal Care Committee.

RNA Pulldown with Mass Spectrometry. STEEL RNA was in vitro transcribed (MEGAscript, Life Technologies). RNA pulldown was performed using the Magnetic RNA-Protein Pull-Down kit (Thermo Fisher Scientific) and eluents were subject to liquid chromatography-tandem mass spectrometry (LC-MS/MS) analysis. The mass spectrometry proteomics data have been deposited to the ProteomeXchange Consortium via the PRIDE (30) partner repository with the dataset identifier PXD008581.

Statistics. Unless otherwise stated, all experiments were performed a minimum of three times, and data represent the mean ± SEM. A P value <0.05 was considered to be statistically significant.

Informed consent from individuals was not required for any protocol in this study and protocols, including tissue culture, are approved by the St. Michael's Hospital Research Ethics Board no. 03–201.

ACKNOWLEDGMENTS. We thank Maria Chalsev for technical support. The human KLF2 promoter was a kind gift from M. Esteller (IDIBELL Bellvitge Biomedical Research Institute, Barcelona). H.S.J.M. is a recipient of a Canadian Institutes of Health Research Training Program in Regenerative Medicine Fellowship; H.S.J.M., A.N.S., P.J.T., K.H.K., and M.K.D. are recipients of the Queen Elizabeth II Graduate Scholarships in Science and Technology. This work was supported by grants from the Canadian Institutes of Health [MOP 142307 (to P.A.M.) and RMF 111624 (to M.V.S.)]. This research was undertaken thanks in part to funding provided to the University of Toronto Medicine by Design initiative by the Canada First Research Excellence Fund.

1. Bhasin M, et al. (2010) Bioinformatic identification and characterization of human endothelial cell-restricted genes. *BMC Genomics* 11:342.
2. Cabili MN, et al. (2011) Integrative annotation of human large intergenic noncoding RNAs reveals global properties and specific subclasses. *Genes Dev* 25:1915–1927.
3. Rinn JL, et al. (2007) Functional demarcation of active and silent chromatin domains in human HOX loci by noncoding RNAs. *Cell* 129:1311–1323.
4. Gupta RA, et al. (2010) Long non-coding RNA HOTAIR reprograms chromatin state to promote cancer metastasis. *Nature* 464:1071–1076.
5. Broadbent HM, et al.; PROCARDIS consortium (2008) Susceptibility to coronary artery disease and diabetes is encoded by distinct, tightly linked SNPs in the ANRIL locus on chromosome 9p. *Hum Mol Genet* 17:806–814.
6. Michalik KM, et al. (2014) Long noncoding RNA MALAT1 regulates endothelial cell function and vessel growth. *Circ Res* 114:1389–1397.
7. Hohl M, Thiel G (2005) Cell type-specific regulation of RE-1 silencing transcription factor (REST) target genes. *Eur J Neurosci* 22:2216–2230.
8. Soshnikova N (2014) Hox genes regulation in vertebrates. *Dev Dyn* 243:49–58.
9. Toshner M, et al. (2014) Transcript analysis reveals a specific HOX signature associated with positional identity of human endothelial cells. *PLoS One* 9:e91334.
10. Fish JE, et al. (2005) The expression of endothelial nitric-oxide synthase is controlled by a cell-specific histone code. *J Biol Chem* 280:24824–24838.
11. Ulitsky I, Bartel DP (2013) lincRNAs: Genomics, evolution, and mechanisms. *Cell* 154:26–46.
12. Kong L, et al. (2007) CPC: Assess the protein-coding potential of transcripts using sequence features and support vector machine. *Nucleic Acids Res* 35:W345–W349.
13. Zhang B, et al. (2014) A novel RNA motif mediates the strict nuclear localization of a long noncoding RNA. *Mol Cell Biol* 34:2318–2329.
14. Chu C, et al. (2015) Systematic discovery of Xist RNA binding proteins. *Cell* 161:404–416.
15. Kohlmaier A, et al. (2004) A chromosomal memory triggered by Xist regulates histone methylation in X inactivation. *PLoS Biol* 2:E171.
16. Ciucurel EC, Sefton MV (2014) Del-1 overexpression in endothelial cells increases vascular density in tissue-engineered implants containing endothelial cells and adipose-derived mesenchymal stromal cells. *Tissue Eng Part A* 20:1235–1252.
17. Wang KC, et al. (2011) A long noncoding RNA maintains active chromatin to coordinate homeotic gene expression. *Nature* 472:120–124.
18. Dekker RJ, et al. (2006) KLF2 provokes a gene expression pattern that establishes functional quiescent differentiation of the endothelium. *Blood* 107:4354–4363.
19. Won D, et al. (2007) Relative reduction of endothelial nitric-oxide synthase expression and transcription in atherosclerosis-prone regions of the mouse aorta and in an in vitro model of disturbed flow. *Am J Pathol* 171:1691–1704.
20. Baeyens N, Bandyopadhyay C, Coon BG, Yun S, Schwartz MA (2016) Endothelial fluid shear stress sensing in vascular health and disease. *J Clin Invest* 126:821–828.
21. Parmar KM, et al. (2006) Integration of flow-dependent endothelial phenotypes by Kruppel-like factor 2. *J Clin Invest* 116:49–58.
22. Chi JT, et al. (2003) Endothelial cell diversity revealed by global expression profiling. *Proc Natl Acad Sci USA* 100:10623–10628.
23. Park H, et al. (2011) Homeobox D1 regulates angiogenic functions of endothelial cells via integrin β1 expression. *Biochem Biophys Res Commun* 408:186–192.
24. Bai P (2015) Biology of poly(ADP-ribose) polymerases: The factotums of cell maintenance. *Mol Cell* 58:947–958.
25. Yan MS, Marsden PA (2015) Epigenetics in the vascular endothelium: Looking from a different perspective in the epigenomics era. *Arterioscler Thromb Vasc Biol* 35:2297–2306.
26. Guo T, et al. (2011) An evolving NGF-Hoxd1 signaling pathway mediates development of divergent neural circuits in vertebrates. *Nat Neurosci* 14:31–36.
27. Yarmishyn AA, et al. (2014) HOXD-AS1 is a novel lncRNA encoded in HOXD cluster and a marker of neuroblastoma progression revealed via integrative analysis of noncoding transcriptome. *BMC Genomics* 15(Suppl 9):S7.
28. Bhattacharya R, et al. (2005) Inhibition of vascular permeability factor/vascular endothelial growth factor-mediated angiogenesis by the Kruppel-like factor KLF2. *J Biol Chem* 280:28848–28851.
29. Bock FJ, Todorova TT, Chang P (2015) RNA regulation by poly(ADP-ribose) polymerases. *Mol Cell* 58:959–969.
30. Vizcaíno JA, et al. (2014) ProteomeXchange provides globally co-ordinated proteomics data submission and dissemination. *Nat Biotechnol* 30:223–226.